

We are IntechOpen, the world's leading publisher of Open Access books Built by scientists, for scientists

6,900

Open access books available

185,000

International authors and editors

200M

Downloads

Our authors are among the

154

Countries delivered to

TOP 1%

most cited scientists

12.2%

Contributors from top 500 universities



WEB OF SCIENCE™

Selection of our books indexed in the Book Citation Index
in Web of Science™ Core Collection (BKCI)

Interested in publishing with us?
Contact book.department@intechopen.com

Numbers displayed above are based on latest data collected.
For more information visit www.intechopen.com



A Facile Method for Formulation of Atenolol Nanocrystal Drug with Enhanced Bioavailability

Luis Castañeda

Abstract

Atenolol is a commonly used antihypertensive drug of class III BCS category. The objective of the present study is to enhance the permeability of atenolol by using a suitable technique which is economical and devoid of using any organic solvents. The nanocrystal technology by high pressure homogenization was chosen for this purpose, which is less expensive and simple method. In this technique, no organic solvent was used. The study was further aimed to characterize prepared nanocrystals in solid state by Fourier-transform infrared spectroscopy (FTIR), powder X-ray diffraction (PXRD) patterns, particle size, zeta potential, % yield, and drug permeation study through isolated goat's intestine. An in vivo study was carried out to determine the pharmacokinetic property in comparison to pure drug powder using rats as experimental animals. The formulation design was optimized by a 3(2) factorial design. In these designs, two factors, namely surfactant amount (X1) and speed of homogenizer (X2), were evaluated on three dependent variables, namely particle size (Y1), zeta potential (Y2), and production yield (Y3).

Keywords: atenolol, nanocrystal, factorial design, ANOVA, antihypertensive, pharmacokinetic

1. Introduction

A nanocrystal is a particle having one or more dimensions of the order of 200 nm or less and considered to have novel characteristics which differentiate them from other materials [1]. When the size of the material is reduced to less than 200 nanometers, the realm of quantum physics takes over and five materials begin to demonstrate entirely new properties. Hence, nanodesign of drugs by various different techniques, like melting, homogenization, and controlled precipitation, is explored to produce drug nanocrystals, nanoparticles, nanosuspensions, etc. [2]. As decrease in size will increase the solubility of drugs, this technology is explored to increase oral bioavailability of sparingly water soluble drugs [3]. Development of soluble and/or permeable drug molecules using nanocrystal formulations has been proven to be successful due to their unique size range and higher surface: volume ratio, which results in enhanced drug dissolution, bioavailability and permeability [4].

Atenolol is a selective β_1 receptor antagonist, a drug belonging to the group of beta blockers, which is used mainly in different cardiovascular diseases [5]. It often

suffers from poor bioavailability after oral dosing due to stumpy permeability through GIT [6]. Approximately 50% of an oral dose is absorbed from the gastrointestinal tract, the remainder being excreted unchanged in the feces. Researchers have been endeavored to increase its permeability and bioavailability by different techniques including osmotic pump, cyclodextrin-based delivery systems, hydrophilic matrices, transdermal delivery systems, and so on [7–12].

In the present study, we had prepared nanocrystals of atenolol to improve its permeability and modify its solubility, because this method is less time-consuming, required no organic solvents or harsh chemicals like other nanodelivery systems, has a high product yield, has good product stability, and is cheap. High pressure homogenization method was employed to prepare nanocrystals [13]. In this method, high pressure was applied on liquid suspension to force it through a gap or narrow channel inside a pipe. Here, the medium was aqueous containing a hydrophilic surfactant SLS to prevent agglomeration of suspended particles and thus it helped in stabilization. The surfactant used in the study also prevented crystal growth (Ostwald ripening) that could change the dissolution and bioavailability of the drug after storage [14].

2. Materials and methods

2.1 Materials

Atenolol was supplied as a gift sample by Haustus Biotech Pvt. Ltd., Himachal Pradesh, India, and sodium lauryl sulfate, manufactured by Krishna Drug and chemical Pvt. Ltd., Gujrat, was supplied by Mahalakshmi Chemicals Ltd., Greater Noida, India. Triple distilled water was used throughout the experiments. All other chemicals were of reagent grade and used without further purification.

2.2 Preparation of atenolol nanocrystals

Atenolol nanocrystals were prepared by high speed homogenization process using sodium lauryl sulfate as a surfactant [15–17]. The nanocrystals were prepared by adding the different compositions of the surfactant sodium lauryl sulfate and stabilizer (PVP K 30) as mentioned in Table 1. Atenolol (1000 mg) was dissolved in

Formulation code	Drug: surfactant	Speed in rpm	Particle size (nm)	Zeta potential (mV)	Production yield
F1	2:1	20,000	312.7 ± 2.0	18 ± 0.2	82 ± 1.0
F2	4:1	20,000	296.7 ± 0.6	20 ± 0.4	88 ± 2.0
F3	4:3	20,000	416.2 ± 0.5	16 ± 0.1	84 ± 1.0
F4	2:1	25,000	210.4 ± 1.0	16.5 ± 0.3	72 ± 0.5
F5	4:1	25,000	125.6 ± 0.5	19 ± 0.2	90 ± 0.8
F6	4:3	25,000	552.6 ± 0.7	17 ± 0.3	88 ± 1.0
F7	2:1	15,000	652.6 ± 2.0	18 ± 0.7	64 ± 1.0
F8	4:1	15,000	620.0 ± 2.5	20 ± 0.4	66 ± 2.0
F9	4:3	15,000	590.0 ± 1.8	19 ± 0.5	64 ± 1.0

Table 1. Formulation composition of atenolol nanocrystal.

80 ml of distilled water with sodium lauryl sulfate which resulted in a solution of 1 g concentration. The whole procedure was operated at $25 \pm 2^\circ\text{C}$. The solution of drug and surfactant was placed under a high-speed homogenizer (T 25 digital ULTRA-TURRAX IKAR Werke Staufen/Germany) at different speeds (15,000–25,000 rpm) for 70 h. The resulting solution was placed in a tray dryer at 60°C to evaporate the solvent. Nanocrystals were collected and evaluated as required.

2.3 Formulation of capsule dosage of atenolol nanocrystals

Atenolol nanocrystals were mixed with the same ratio of lactose powder, which shows no incompatibility with the drug. The mixture of 1:1 ratio of drug (atenolol nanocrystals) and lactose was prepared. Then, 100 mg of this mixture was filled into the capsules.

3. Characterization of nanocrystals

The nanocrystals of atenolol prepared by the abovementioned method was characterized by the following techniques.

3.1 Particle size and zeta potential analysis

Particle size of the prepared nanocrystals was determined using particle size analyzer (Malvern Instruments Ltd.). The prepared nanocrystals were dispersed in dimethyl sulfoxide and placed in cuvettes and the particle size in terms of average diameter (davg) was determined. Zeta potential was calculated by using Zetasizer ZS 90 (Malvern Instrument Ltd. India) [18].

3.2 Scanning electron microscopy

The morphology of the atenolol nanocrystals was examined by scanning electron microscopy (JSM 6390 India). The sample was mounted on to an aluminum stub and sputter coated for 120 s with platinum particles in an argon atmosphere. The coated samples were then scanned and images were analyzed at 500 or 1000 axis [18].

3.3 Fourier-transform infrared (FTIR) analysis

FTIR analysis of pure atenolol, mixture of atenolol and SLS and obtained nanocrystals and lactose was performed in the range of $4000\text{--}500\text{ cm}^{-1}$ as thin KBr pellets using FTIR spectrophotometer (Perkin-Elmer BX II). The observed peaks were reported for functional groups.

3.4 X-ray diffraction study (XRD)

The crystallinities of atenolol and atenolol nanocrystals were evaluated by XRD measurement using an X-ray diffractometer (Bruker AXS, 08 Advance). All samples were measured in the 2θ angle range between 3 and 80° and 0.010 step sizes.

3.5 Percentage yield of production

For any formulation, it is always desirable to have a better production yield so that industrial production becomes feasible not only in terms of cost but also in

terms of environmental protection. The production yield of prepared nanocrystals was calculated by the following Eq. (1):

$$\text{Percentage yield} = (B/A) \times 100 \quad (1)$$

where B is the weight percentage of the final product obtained after drying, and A is the initial total amount of atenolol and sodium lauryl sulfate used for the preparation.

3.6 In vitro release studies of atenolol nanocrystals

The dissolution test was performed in the USP type II apparatus. Nanocrystals (100 mg) were accurately weighed and put into the pretreated dialysis membrane and sealed with clips. The release medium was phosphate buffer (pH 6.8) maintained at 37°C with agitation rate set at 50 rpm. The amount of drug was determined spectrophotometrically at $\lambda_{\text{max}} = 275$ nm against suitable blank using a preconstructed calibration curve [19].

3.7 In vitro release studies of capsule dosage form of atenolol nanocrystals

The dissolution test was performed on the USP type I apparatus. Capsules containing nanocrystals (100 mg) were accurately placed into the basket of dissolution test apparatus. The release medium was phosphate buffer (pH 6.8) maintained at 37°C with agitation rate set at 50 rpm. The amount of drug released was determined spectrophotometrically at $\lambda_{\text{max}} = 275$ nm.

3.8 In vitro intestinal permeability studies of pure atenolol and atenolol nanocrystals

The permeability studies of pure atenolol and atenolol nanocrystals were carried out using Franz diffusion cell. To check the intra duodenal permeability, the duodenal part of the small intestine was isolated from sacrificed goat and taken for the in vitro diffusion study. Then this tissue was thoroughly washed with cold Ringer's solution to remove the mucous and lumen contents. The sample solutions were injected into the lumen of the duodenum using a syringe, and the two sides of the intestine were tightly closed. Then the tissue was placed in a chamber of organ bath with continuous aeration and at a constant temperature of 37°C. The receiver compartment was filled with 30 mL of phosphate-buffered saline (pH 5.5). The permeability was tested for 60 minutes. The absorbance was measured using a UV-Vis spectrophotometer at a wavelength of 275 nm, keeping the respective blank. The percent diffusion of the drug was calculated against time and plotted on a graph.

3.9 Stability studies of prepared nanocrystals

The prepared nanocrystals were subjected to stability studies. The nanocrystals were placed in stability chambers for a month at different temperatures, like 4, 25, 37, and 60°C. After 1 month, the tested nanocrystals were subjected to FTIR to find the spectra and compare with the standard spectra of nanocrystals.

3.10 In vivo studies

To determine the in vivo pharmacokinetic parameters for optimized nanocrystal formulation, experimental rats were used. This investigation adhered to the Principles of Laboratory Animal Care. Female albino rats (0.20–0.25 Kg) were

Drug: surfactant (X1)	Speed in rpm (X2)
−1	1
0	1
1	1
−1	0
0	0
1	0
−1	−1
0	−1
1	−1
−1 = 2:1	−1 = 15,000
0 = 4:1	0 = 20,000
+1 = 4:3	+1 = 25,000

Table 2.
Design of experiment for 3² factorial analysis.

divided in two groups, each containing six. They were fasted overnight and allowed to administer 0.5 mL aqueous dispersion of pure drug and the most successful formulation of nanocrystal (equivalent to 10 mg/mL atenolol) using oral feeding tube. Blood samples of 0.2 mL were withdrawn through the tail vein of rats after 0.5, 1, 1.5, 2, 2.5, 4, 6, and 24 h of sample administration. The withdrawn samples were centrifuged at 5000 rpm for 20 min. The plasma was separated and stored at −20°C until drug analysis was carried out using HPLC analytical method of analysis. The whole process was carried out according to the reported method by Anwar et al. [20].

3.11 Statistical analysis

Independent T-test was used to analyze data of two batches obtained in various experiments at the 0.05 level of significance by Origin 6.0 software. The difference was considered significant at $p \leq 0.05$.

3.12 Experimental design and statistical analysis

In this study, a 32 full factorial experimental design was introduced to optimize the formulation of nanoparticles. Initial studies were undertaken to decide on the factors and their levels in the experimental design. Based on the results obtained in preliminary experiments, surfactant amount and speed of homogenizer were found to be the major variables in determining the particle size and production yield. So, in this design, two factors, namely surfactant amount (X1) and speed of homogenizer (X2), were evaluated each at three levels and suitably coded (**Table 2**). The effect of these factors were evaluated on three dependent variables, namely particle size (Y1), zeta potential (Y2), and production yield (Y3). A total of 9 formulations were prepared with these variables.

For the studied design, the multiple linear regression analysis (MLRA) method was applied using Statistica 10 (StatSoft Inc., USA) software to fit the full second-order polynomial equation with added interaction terms. Polynomial regression results were demonstrated for the studied responses using Eq. (2):

$$Y = b_1 + b_2X_1 + b_3X_2 + b_4X_1X_2 + b_5X_1^2 + b_6X_2^2 \tag{2}$$

where Y is the dependent variable and b1 is the arithmetic mean response of the 9 trials. Coefficient b2 is the estimated coefficient for the factor X1, and coefficient b3 is the estimated coefficient for the factor X2. The main effects (X1 and X2) represent the average result of changing one factor at a time from its low to high value. The interaction terms (X1X2) show how the response changes when two factors interact. The polynomial terms (X1² and X2²) are included to investigate nonlinearity. The values of correlation coefficients were set to be statistically significant at 95% confidential interval [21]. To analyze the significance level of all these data, ANOVA was used at 95% confidence interval at 0.05 significance level.

4. Results and discussion

4.1 Characterization of drug, excipients, and their interactions by FTIR

FTIR spectroscopy was used to further characterize possible interactions between the drug and the excipients. The FTIR spectra of atenolol and sodium lauryl sulfate and also of the formulated nanocrystals and lactose were obtained at wavelength ranging from 4000 to 400 cm^{-1} . The spectra obtained from FTIR studies confirmed that there was no major shifting, as well as no loss of functional peaks between the spectra of pure atenolol and atenolol nanocrystals. Comparing the spectra of pure atenolol and atenolol nanocrystals, no difference was shown in the position and trend of the absorption bands. All the distinctive groups in the FTIR spectra of atenolol were found in all the spectra of atenolol nanocrystals, like the amide group ($\text{O}=\text{C}-\text{NH}_2$) extruding from the benzene ring. Apart from the amide functional group, the presence of the conjugating $\text{C}=\text{C}$ bond in the benzene ring, the methane (CH), methylene (CH_2) methyl (CH_3), and OH functional group were distinctly observed in the IR spectra (amide: 1650 cm^{-1} ; CH: $2880-2900 \text{ cm}^{-1}$; CH_2 : $2916-2936 \text{ cm}^{-1}$; CH_3 : 2850 cm^{-1} ; conjugating $\text{C}=\text{C}$: $1640-1610 \text{ cm}^{-1}$; OH: $3200-3550 \text{ cm}^{-1}$), thus providing evidence for the absence of any chemical incompatibility between SLS and atenolol.

4.2 Particle size and zeta potential

The particle size of the atenolol nanocrystal formulations shown in **Table 1** showed a narrow size distribution from 125 to 652 nm, where the intensity of 117.8 nm was 93% and that of 652.5 nm was only 7%. The effect of stirring speed had an enormous effect on particle size. Formulation prepared with 25,000 rpm had smaller size as compared to particle prepared with 15,000 rpm. Concentration of SLS also had an effect on the size distribution. Less concentration of SLS yielded smaller size particles. The formulated nanocrystals were positively charged (16–19 mV), which is desirable for good ocular interaction. Formulation F7 was not further considered due to its larger size (more than 650). This may be due to slow stirring speed.

4.3 Production yield

The date of percentage yield of the prepared nanocrystals (**Table 1**) showed that the atenolol-SLS nanocrystals (batch F5), prepared by drug:SLS ratio 4:1, had comparatively higher yield of production (90%). Stirring speed and concentration of SLS also had an effect on the production yield.

4.4 Scanning electron microscopy

The SEM image, as shown in **Figure 1**, of the atenolol nanocrystals revealed that the particles were crystalline in shape. The average size of the atenolol nanocrystals was found to be less than 200 nm, which was further supported by the results of particle size analysis by Zetasizer.

4.5 X-ray diffraction (PXRD) studies

The powder X-ray diffractogram of pure atenolol powder from 5 to 50° 2 θ showed numerous distinctive peaks at 2 θ degree that indicated a high crystalline content. The samples were scanned for 2 θ values over a range from 5 to 50°C at a scan rate of 10°/min. The PXRD pattern of pure drug and atenolol nanocrystals were compared with regard to peak positions and relative intensities and presence and/or absence of peaks in certain regions. **Figure 2** represents the XRD photograph of different nanocrystal formulation and pure atenolol powder.

4.6 Permeability study

The permeability study showed increased permeability, when the atenolol was converted into the nanocrystals. The diffusion study showed that the % permeability of nanocrystal formulations was much higher as compared to that of the pure drug. The formulation F5 showed the maximum % release of 90.88%, whereas the pure drug showed only 31.22% release **Figure 3**.

4.7 In vitro dissolution studies

The dissolution rate of pure atenolol was very poor and during a 120-min period, 51.64% of drug was released. The reason for the poor dissolution of pure drug could be poor wettability and poor solubility. In vitro release studies revealed that there was a marked increase in the dissolution rate of atenolol, in the range of 78.30–98.28%, from all nanocrystal formulation compared to pure atenolol. The results revealed that the nanocrystals with a ratio of drug to carrier, 4:1, were having a higher dissolution rate in comparison to all other ratios. This could be attributed to the hydrophilic character of the surfactant and to the amorphous state of the drug. Hence, the present study showed that nanocrystal formulation can

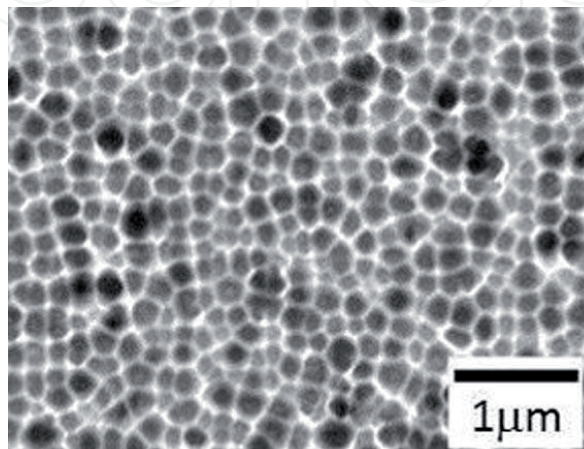


Figure 1.
SEM images of atenolol nanocrystals.

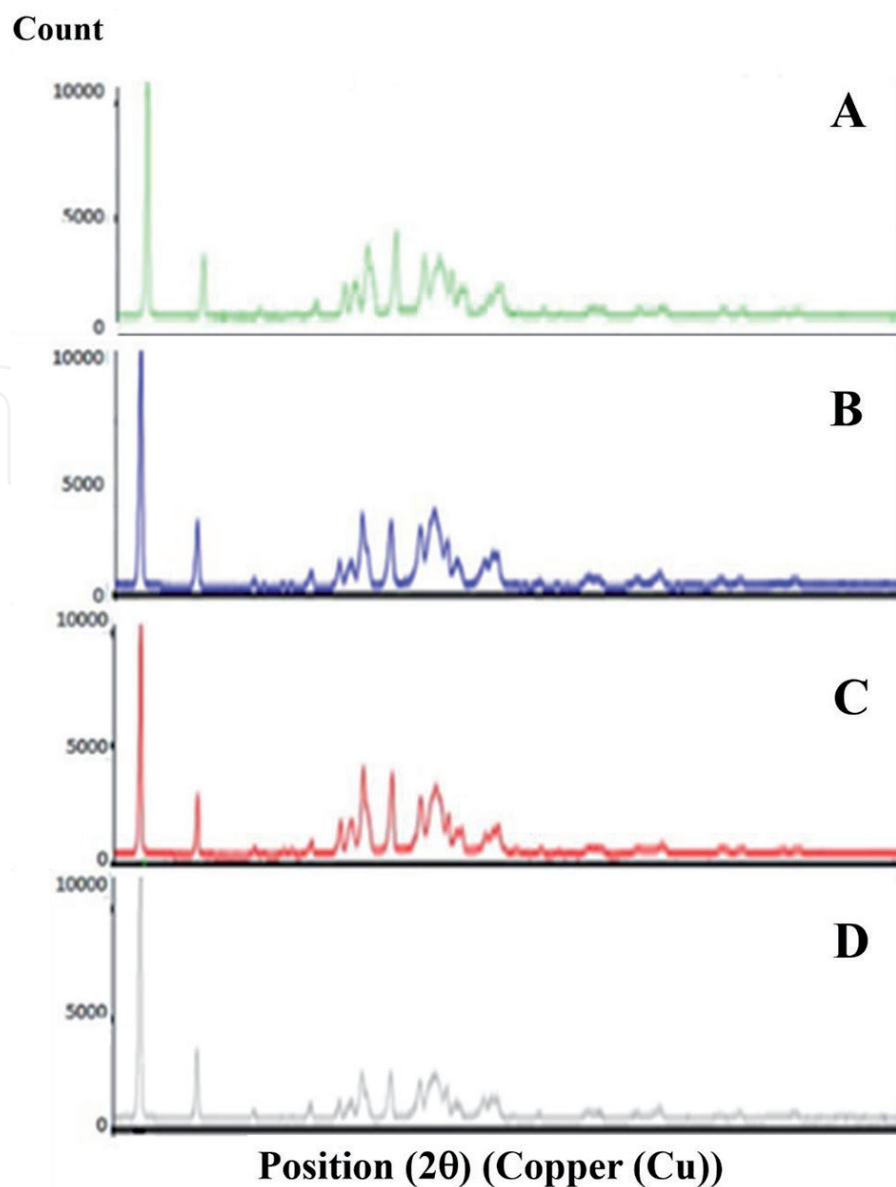


Figure 2.
XRD of atenolol nanocrystals F5 (A), atenolol pure drug (B), atenolol nanocrystals F4 (C), and nanocrystals F1 (D).

be successfully used to enhance dissolution rate of poorly soluble drugs. **Figure 4** shows drug release profile of pure drug nanocrystal formulation [F5] and capsulated nanocrystals.

4.8 Stability studies

The physical appearance of the prepared nanocrystals after keeping them 1 month in stability chambers under various conditions was found to be white to off-white in color, odorless, and crystalline powder. FTIR spectroscopy was used to further characterize possible interactions between the drug and the excipients during the stability studies. There was no major change shown in the FTIR peaks. The prepared nanocrystal formulation was stable during the stability studies done for 1 month.

4.9 In vitro study

The results of in vivo study revealed an improvement in bioavailability of nanocrystal formulation; it was observed that after oral dosing of the drug and the equation 3, their

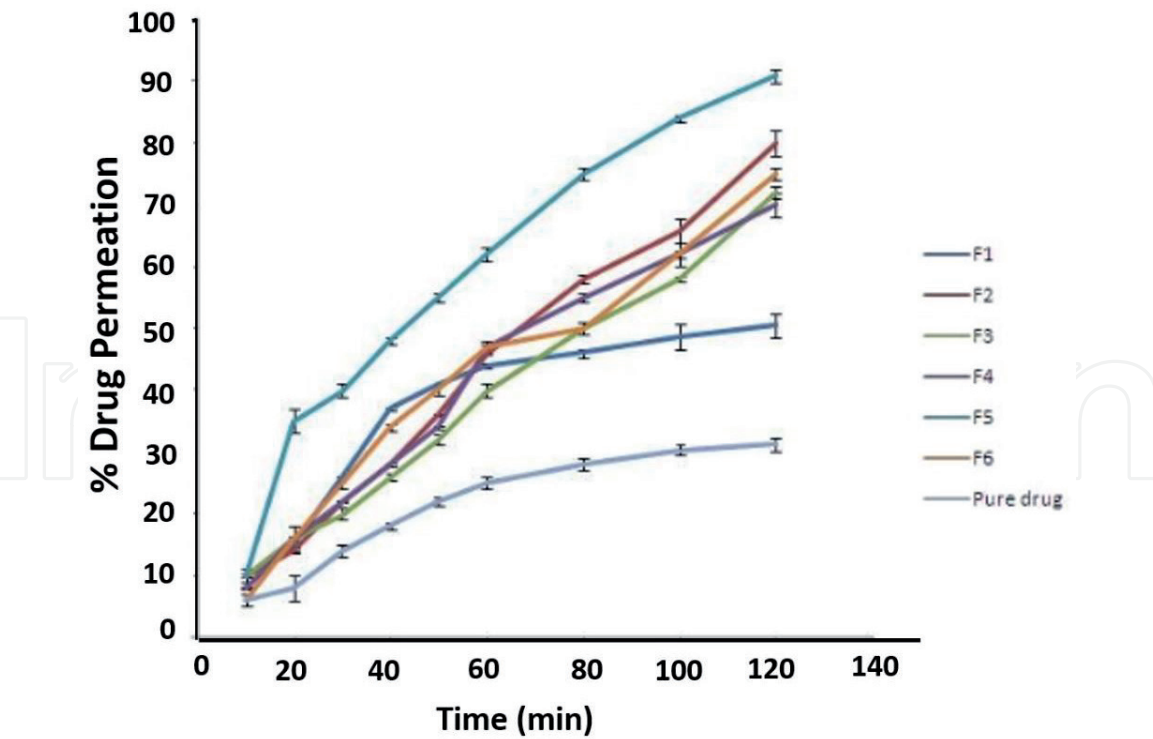


Figure 3.
Permeability from Franz diffusion cell of atenolol pure drug and atenolol nanocrystal formulations.

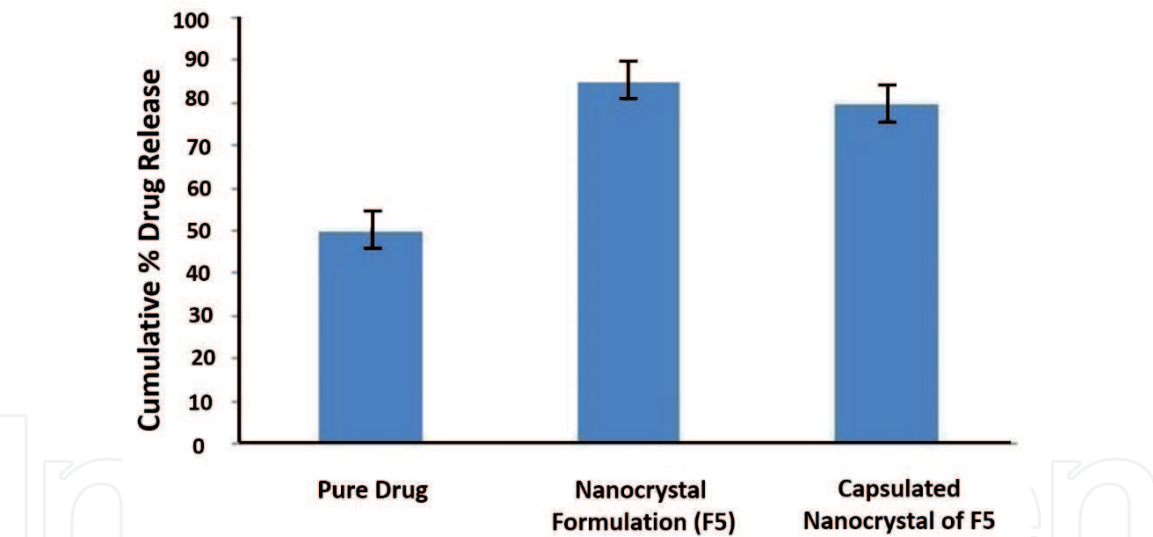


Figure 4.
In vivo dissolution cumulative of % release of atenolol pure drug, atenolol nanocrystals F5, and capsule dosage of nanocrystals in phosphate buffer (pH 6.8).

individual kinetic curve exhibited double peaks. Thus, double peaks can be due to the existence of two absorption sites in the gut interrupted by a region of poor absorption [21]. A rapid attainment of peak plasma concentrations was observed that may be due to the burst release effect brought by the use of SLS for stabilization of nanocrystals. Same phenomenon was reported by Vergote et al. [22]. The AUC0–24 h, MRT, and C_pmax for test formulation were significantly higher at $p < 0.05$ compared to the drug (Table 3).

4.10 Factorial analysis

Applied 3² factorial design yields coefficient for one factor and for two factors as well. Coefficient for more than one factor represents interaction of both factors.

Formulation	Cpmax (µg/mL)	Tmax (hour)	AUC0–24 (mAU)	MRT (hour)
Pure drug	612.15 ± 10.6	5.2 ± 1.4	26927.8 ± 4.2	46.56 ± 3.1
Nanocrystal formulation	957.51 ± 20.4	2.8 ± 0.5	75329.3 ± 6.3	84.64 ± 4.6

Table 3.
Pharmacokinetic data of nanocrystal formulation and pure drug.

Coefficient may be positive or negative for synergistic or antagonistic effect, respectively. The coefficients can be directly compared to assess the impact of factors on responses. Obtained polynomial Eqs. (3)–(5) for dependent variables are as follows:

$$\begin{aligned} \text{Particles Size} = & 4280.7153 - 6169.2601 \times x - 0.2812 \times y + 4894.7164 \\ & \times x \times x + 0.1959 \times x \times y + 4.6667E^{-8} \times y \times y \end{aligned} \tag{3}$$

$$\begin{aligned} \text{Zeta potential} = & 31.4304 - 43.3651 \times x - 0.0004 \times y + 67.3401 \\ & \times x \times x - 0.0004 \times x \times y + 1E^{-8} \times y \times y \end{aligned} \tag{4}$$

$$\begin{aligned} \text{Production Yield} = & -71.7445 - 370.4401 \times x + 0.0192 \times y + 606.0606 \\ & \times x \times x - 0.0009 \times x \times y - 4.2667E^{-7} \times y \times y \end{aligned} \tag{5}$$

Speed of homogenizer has a greater effect on the particle size (−0.2812), zeta potential (−0.0004), and production yield (0.0192), whereas amount of surfactant has a lesser effect on the production yield (−370.4401), zeta potential (−43.3651), and particle size (−669.2601).

It was clearly depicted from the magnitude of the coefficients that the amount of surfactant has a positive effect on all the three variables including particle size, zeta potential, and production yield; whereas, the magnitude of the coefficients for speed of homogenizer has an antagonistic effect on all the three variables.

Contour plots and surface plots as shown in **Figures 5** and **6** were plotted, which are very useful to study the interaction effects of the factors on the responses. The response surface depicts the effect of factor contributions at different levels on studied response. Three contour parameters were established for particle size. Drug entrapment and drug release percentage. The contour plots showed very clearly the relationship between the independent variables and the responses.

P value for the effect of drug surfactant ratio is statistically insignificant for particle size and production yield *p* has value greater than 0.05, but it is significant only for zeta potential (*p* = 0.009851) and particle size (*p* = 0.035269). Speed of homogenizer has an insignificant effect on zeta potential.

The goodness of fit of the R^2 model was checked by the determination coefficient (R^2). The values of the determination coefficients for particle size ($R^2 = 0.78297$), zeta potential ($R^2 = 0.80392$), and production yield ($R^2 = 0.8988$) indicated that over 95% of the total variations are explained by the model. The values of adjusted determination coefficients (adj $R^2 = 0.56594$ for particle size, 0.60784 for zeta potential, and 0.79761 for production yield) are also very high (over 90% of the total variations), which indicates a high significance of the model.

A good way to check the model is to enter factor levels from the experimental design (observed response) and generate the predicted response. When we compare the predicted value with actual value, a discrepancy occurs which is called residual.

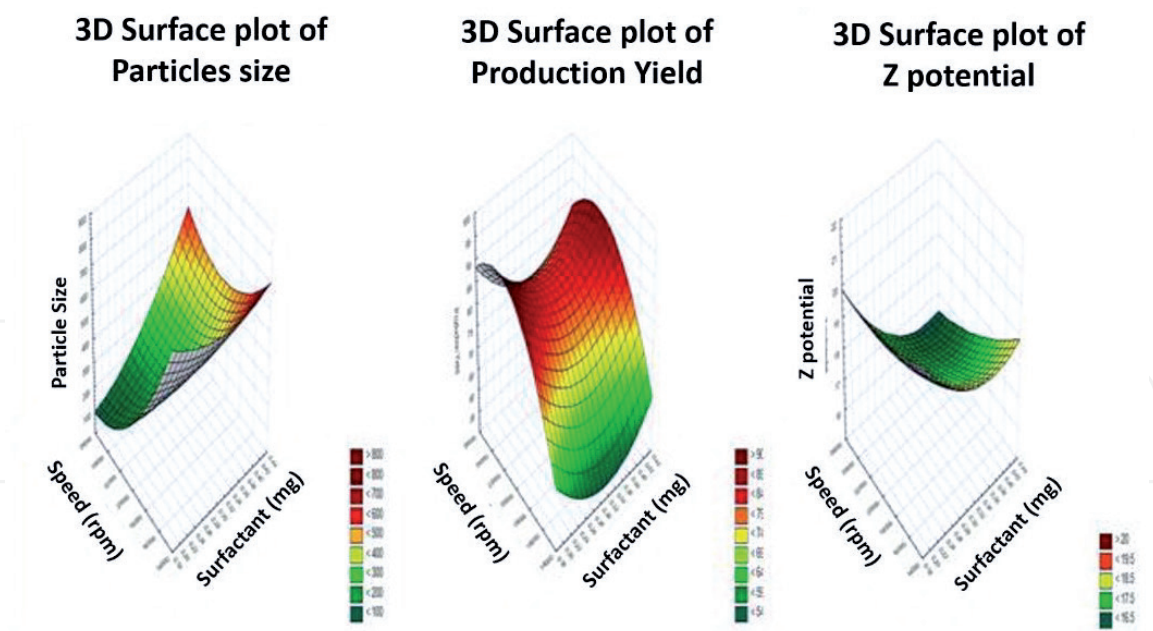


Figure 5.
3D surface plots for the different variables (in order of particle size, production yield, and zeta potential).

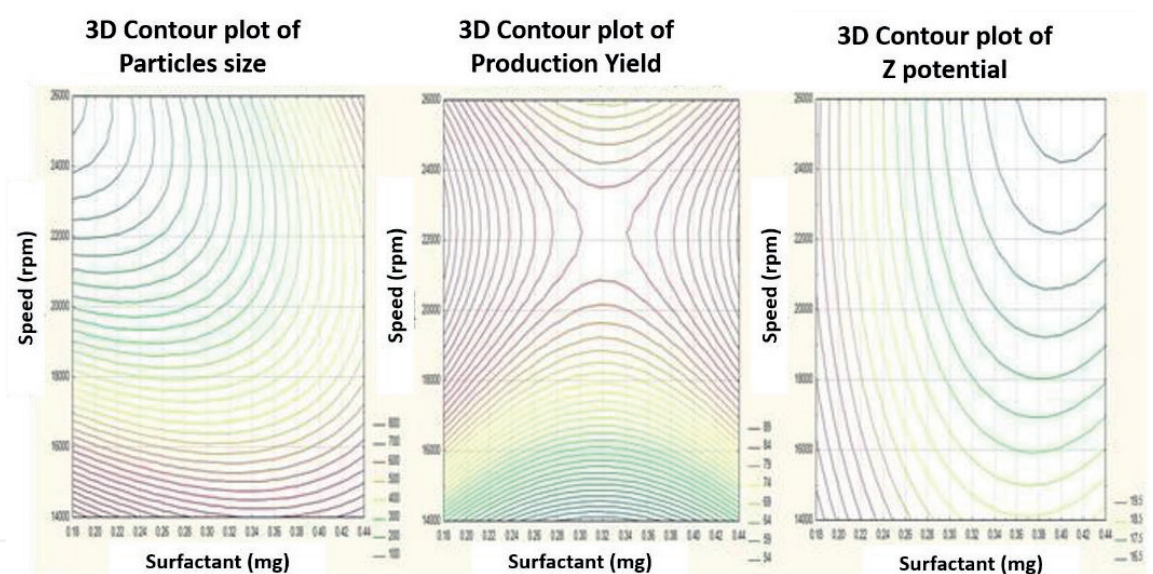


Figure 6.
3D contour plots for the different variables (in order of particle size, production yield, and zeta potential).

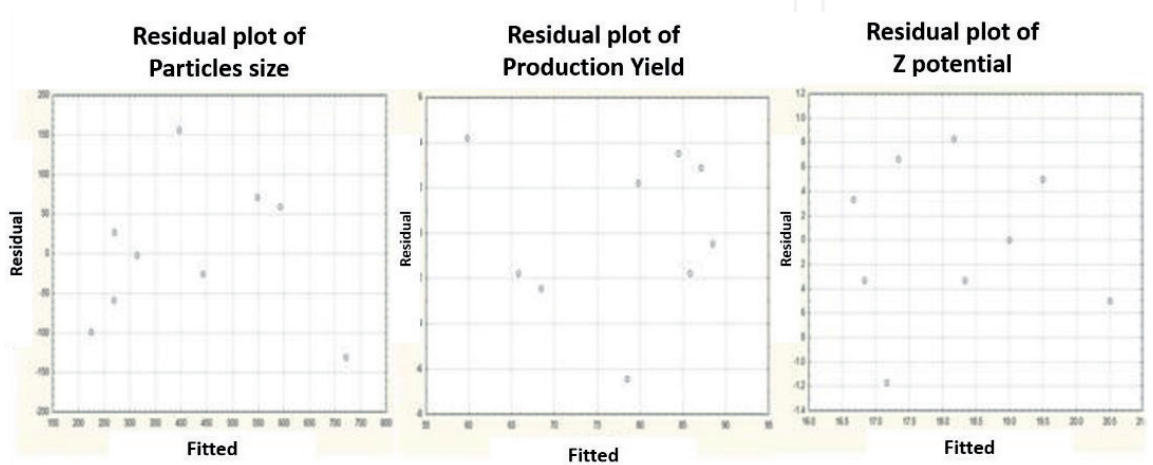


Figure 7.
Plots of residuals for the three different variables (in order of particle size, production yield, and zeta potential).

For statistical purposes, it is assumed that the residuals are normally distributed and independent with constant variance [21]. Residual versus predicted plots were constructed to check the statistical assumptions. In this experiment, there is no definite increase in residuals with predicted levels, which support the underlying statistical assumptions of constant variance. Moreover, the obtained plots of residuals that do not exhibit any systematic structure indicate that the model fits the data well (**Figure 7**). Plots of the residuals versus other predictor variables, or potential predictors that exhibit systematic structure indicate that the form of the function can be improved in some ways.

5. Conclusions

In this study, atenolol nanocrystals had been developed successfully by high-speed homogenization and simultaneous drying, which have shown an improved dissolution and permeability behavior compared to that of the pure drug. Statistical analysis revealed speed of homogenizer had bigger effect on the three observed parameters, whereas amount of surfactant had a lesser effect on them. SEM pictures had shown that the size of the particles obtained after homogenization is below 1 μm . This implied that the size of the drug crystals in these particles was of nanoscale. Therefore, it can be concluded that the selected method of nanocrystal formation and its further optimization by factorial design was effective to increase the solubility, as well as permeability of atenolol.

Acknowledgements

The authors gratefully acknowledge the financial support from the Graduate Studies and Research Section of the Higher School of Medicine, National Polytechnic Institute, through project No. 20190031.

Conflict of interest

The author declares no conflict of interest.


Author details

Luis Castañeda

Sección de Estudios de Posgrado e Investigación de la Escuela Superior de Medicina, Instituto Politécnico Nacional, Plan de San Luis y Díaz Mirón S/N, Casco de Santo Tomas, Cd. de México, Mexico

*Address all correspondence to: lcastaneda@ipn.mx

IntechOpen

© 2019 The Author(s). Licensee IntechOpen. This chapter is distributed under the terms of the Creative Commons Attribution License (<http://creativecommons.org/licenses/by/3.0>), which permits unrestricted use, distribution, and reproduction in any medium, provided the original work is properly cited. 

References

- [1] Fichera MA, Keck CM, Muller RH. Nanopure technology-drug nanocrystals for the delivery of poorly soluble drugs. In particles; 2004
- [2] Pace GW. Process to generate submicron particles of water insoluble compounds. US Patent 6-177-103; 2001
- [3] Bushrab NF, Muller RH. Nanocrystals of poorly soluble drugs for oral administrations. *New Drugs*. 2003;5:20-22
- [4] Srivalli KMR, Mishra B. Drugs nanocrystals: A way toward scale-up. *Saudi Pharmaceutical Journal*. 2016;24(4):384-404
- [5] Wander GS, Chhabra ST, Kaur K. Atenolol drug profile. Supplement: *Journal of Association of Physicians of India*. 2009;57:13-16
- [6] Wu F, Cheni P, Lee YJ, Long RR. Comparative pharmacokinetics of two atenolol products. *Journal of Food and Drug Analysis*. 2003;11(1):4-7
- [7] Singh B, Kaur S, Chakkal AN. Formulation and optimization of controlled release mucoadhesive tablets of atenolol using response surface methodology. *AAPS PharmSciTech*. 2006;7:E19-E28
- [8] Vaithiyalingam SR, Sastry SV, Dehon RH, Reddy LK, Khan MA. Long-term stability characterization of a controlled release gastrointestinal therapeutic system coated with cellulose acetate pseudolatex. *Pharmazie*. 2001;56:66-69
- [9] Kim J, Shin SC. Controlled release of atenolol from the ethylene-vinyl acetate matrix. *International Journal of Pharmaceutics*. 2004;273:23-27
- [10] Jug M, Becirevic-Lacan M, Bengez S. Novel cyclodextrin-based film formulation intended for buccal delivery of atenolol. *Drug Development and Industrial Pharmacy*. 2009;35:796-807
- [11] Kulkarni A, Bhatia M. Development and evaluation of regioselective bilayer floating tablets of atenolol and lovastatin for biphasic release profile. *Iranian Journal of Pharmaceutical Research*. 2009;8:15-25
- [12] Srivastava AK, Wadhwa S, Ridhurkar D, Mishra B. Oral sustained delivery of atenolol from floating matrix tablets-formulation and in vitro evaluation. *Drug Development and Industrial Pharmacy*. 2005;31:367-374
- [13] Kobierski S, Hanisch J, Mauludin R, Muller RH, Keck C. Nanocrystal production by smartcrystal combination technology. *International Symposium on Controlled Release of Bioactive Materials*. 2008;35:3239
- [14] Loh ZH, Samanta AK, Heng PWS. Overview of milling techniques for improving the solubility of poorly water-soluble drugs. *Asian Journal of Pharmaceutical Sciences*. 2015;19:255-274
- [15] Merisko-Liversidge E, Liversidge GG, Copper ER. Nanosizing: A formulation approach for poorly-water-soluble compounds. *European Journal of Pharmaceutical Sciences*. 2003;18:113-120
- [16] Akkar A, Muller RH. Nanocrystals of itraconazole and amphotericin B produced by high pressure homogenization. In: *Annual Meeting of the American Association of Pharmaceutical Scientists*. Valencia/ USA: American Scientific Publishers; 2003. pp. 479-491
- [17] Mauludin R, Möschwitzer J, Müller RH. Comparison of ibuprofen drug nanocrystals produced by high

pressure homogenization (HPH) versus ball milling. AAPS Annual Meeting. Nashville; 2005. p. T2217

[18] Singh A, Deep A. Formulation and evaluation of nanoparticles containing atenolol. *International Journal of Pharmaceutical Research*. 2011;**3**:59-62

[19] Moneghini M, Carcano A, Zingone G, Perissutti B. Studies in dissolution enhancement of atenolol. *International Journal of Pharmaceutics*. 1998;**175**:177-183

[20] Anwar M, Warsi MH, Mallick N, Akhter S, Gahoi S, Jain GK, et al. Enhanced bioavailability of nano-sized chitosan-atorvastatin conjugate after oral administration to rats. *European Journal of Pharmaceutical Sciences*. 2011;**44**:241-249

[21] Mummaneni V, Dressman JB, Amidon GL. Gastric pH influences the appearance of double peaks in the plasma concentration-time profiles of cimetidine after administration in dogs. *Pharmaceutical Research*. 1995;**12**:780-786

[22] Vergote GJ, Vervaet C, Van Driessche I, Hoste S, De Smedt S, Demeester J, et al. In-vivo evaluation of matrix pellets containing nanocrystalline ketoprofen. *International Journal of Pharmaceutics*. 2002;**240**:79-84